J Mater Sci (2010) 45:418–428
DOI 10.1007/s10853-009-3957-y

# Kinetic parameters during the tempering of low-alloy steel through the non-isothermal dilatometry

**J. A. V. Leiva · E. V. Morales · E. Villar-Cociña · C. A. Donis · Ivani de S. Bott**

Received: 16 April 2009 / Accepted: 5 October 2009 / Published online: 22 October 2009


**Abstract** The kinetic study of the tempering reactions of a low-alloy steel (AISI 1050) was carried out through non-isothermal dilatometry. The kinetic parameters of the first and third stages on tempering (here referred to as processes I and II) are calculated by procedures which assume that the nucleation and growth reactions obey a Kolmogorov–Johnson–Mehl–Avrami (KJMA) kinetic model. The recipes to obtain the kinetic parameters ($E$, $K_0$, $n$) of the reactions on tempering are presented. The first stage of tempering is characterized by the growth of the transition carbide nuclei formed during the quenching, $n = 1$ (site saturation situation). This stage is controlled by the pipe diffusion of the iron atoms. The third stage of tempering is characterized by the cementite nucleation on dislocations due to the gradual dissolution of the transition carbide, $n = 0.66$. The cementite growth is controlled by diffusion of the iron atoms through dislocations and in the matrix.

J. A. V. Leiva · E. V. Morales (✉) · E. Villar-Cociña
Department of Physics, Las Villas Central University, Carretera a Camajuani Km. 5.5, CP 54830 Santa Clara, Villa Clara, Cuba
e-mail: evalen@uclv.edu.cu

C. A. Donis
Computer Science Department, Las Villas Central University, Carretera a Camajuani Km. 5.5, CP 54830 Santa Clara, Villa Clara, Cuba

I. de S. Bott
Department of Materials Science and Metallurgy, Catholic University of Rio de Janeiro, Rua Marques de S. Vicente 225, Gávea, Rio de Janeiro, RJ CEP 222541-900, Brazil

## Introduction

The goal of modeling a thermally activated reaction in the solid state is the derivation of a complete description of the progress of a reaction that is valid for any thermal treatment (isothermal, by linear heating, or any other non-isothermal treatment) [1].

It is well established in the literature [2–5] to assume that the transformation rate during a reaction in many solid systems is the product of two functions; one depending solely on the temperature ($T$), and the other depending solely on the fraction transformed ($\xi$):

$$\frac{d\xi}{dt} = K(T) * g(\xi), \tag{1}$$

where $g(\xi)$ is a specific function of the fraction transformed and $K(T)$ is the rate constant of the reaction mechanism. This $K(T)$ is assumed to have Arrhenius temperature dependence:

$$K(T) = K_0 \exp\left[-\frac{E}{RT}\right]. \tag{2}$$

In Eq. 2, $E$, $K_0$, and R are the activation energy of the reaction mechanism, the frequency factor, and the gas constant, respectively.

In the past, a number of methods have been proposed to describe the progress of a reaction in solid systems from non-isothermal experiments. Although non-isothermal experiments can use any arbitrary thermal history, the most usual in thermal analysis is to employ a constant heating rate ($\beta = dT/dt = \text{const}$).

In order to study the kinetics of the phase transformations performed at constant heating rates ($\beta$), a wide range of methods has been established for deriving the kinetic parameters of the reactions obeying Eqs. 1 and 2 [1]. Thus,

without recourse to any kinetic model, values for effective activation energy can be obtained upon isochronal experiments from the temperatures $T_\xi$ needed to attain a certain fixed value of $\xi$ (temperatures corresponding to the same degree of transformation), as measured for different heating rates ($\beta$) [6]. The procedures that use the above temperatures $T_\xi$ for calculating the effective activation energy are known as Kissinger-like methods [1, 6], and these rely on approximating the so-called temperature integral [6–9]. Another set of methods does not use any mathematical approximation for calculating the temperature integral, but instead require determinations of the reaction rates at a stage with the same degree of transformation (it corresponds to an equivalent stage of the reaction) for various heating rates. These procedures are known as the Friedman-like methods [10].

As the determination of $g(\xi)$, $E$, and $K_0$ (the so-called kinetic triplet) are an interlinked problem in non-isothermal experiments [1, 11], a deviation in the determination of any of the three will cause a deviation in the other parameters of the triplet. Thus, it is important to start the analysis of a non-isothermal experiment by determining one element of the triplet with high accuracy. In this sense, it is usual to calculate the effective activation energy ($E$) by a Kissinger-like method for nucleation and growth reactions [6, 12, 13]. This is because the $T_\xi$ constitutes a parameter that can be determined with high accuracy in non-isothermal dilatometric experiments. For nucleation and growth reactions, in general, the effective activation energy is a function of both transformation time and temperature ($E$ does not have to be constant even with constant nucleation and growth mechanisms). Because of this, the above lineal approximation of the Kissinger-like plot will be strictly valid only if the effective activation energy is constant during the entire transformation [13]. This condition is initially ignored in most articles. Thus, this article has been devised to explore the possibilities that combination of the different non-isothermal analysis methods has to obtain the kinetic parameters of the tempering reactions in low-alloy steels using non-isothermal dilatometric data. The determination of the effective activation energy according to a Kissinger-like plot is treated [6, 12]. Thereafter, it is determined if the effective activation energy is constant during the entire transformation using a procedure detailed in [14] that has been modified in this article to nucleation and growth reactions obeying a KJMA kinetic model. Besides, the Avrami exponent ($n$) is calculated with enough accuracy without the influence of some approximations used by other authors (e.g., Ref. [12]). The frequency factor $K_0$ is also obtained as it is outlined below. These recipes allow characterizing the precipitation reactions on tempering in low-alloy steels.

## Non-isothermal dilatometric analysis: theoretical background

The precipitation reactions which occur on tempering of low-alloy steels may all be classified as nucleation and growth reactions [15]. These transformations in isothermal conditions are generally described by the KJMA relation [16–18]:

$$\xi = 1 - \exp -(\theta)^n \text{ with } \theta = K(T)\, t, \tag{3}$$

where $n$ is known as the Avrami exponent and $t$ is the time.

The degree of transformation $\xi$ (fraction transformed) as a function of the physical property $p$, measured during the curse of transformation, is commonly defined by:

$$\xi = \frac{p - p_0}{p_1 - p_0}, \tag{4}$$

where $p_0$ and $p_1$ correspond with the values of $p$ at start and finish stages of the transformation, respectively. In non-isothermal analysis $p_0$ and $p_1$ depend on temperature [6].

In order to maintain the KJMA description under non-isothermal conditions, the formalism of Eq. 3 is accepted for an infinitesimal lapse of time [12, 19], where Eq. 2 has been considered:

$$\mathrm{d}\theta = K_0 \exp\left(-\frac{E}{R * T}\right) \mathrm{d}t. \tag{5}$$

Integration of Eq. 5 resulted in:

$$\theta(T) = \frac{T^2}{\beta}\frac{R}{E}\left(K_0 \exp\left[-\frac{E}{RT}\right]\right)\left(1 - \frac{2RT}{E}\right), \tag{6}$$

where at the initial temperature $T_0 (T_0 \ll \mathrm{T})$ it is assumed that $\theta(\mathrm{T_0}) = 0$.

After deriving Eq. 4 twice with respect to $T$, evaluating the resulted equation at temperatures corresponding to the inflection points $T_\mathrm{i}$ (the temperatures belonging to the inflection points ($T_\mathrm{i}$) in the dilatometric records at various heating rates occur to a vary good approximation at the same degree of transformation [6]), and taking into account several mathematical approximations, the authors of the articles [12, 19] finally obtained the working expression:

$$\ln\left[\frac{\beta}{T_\mathrm{i}^2}\right] = -\frac{E}{R * T_\mathrm{i}} + \ln\left[\frac{RK_0}{E}\right] - \mathrm{Res1} - \mathrm{Res2}, \tag{7}$$

with

$$\mathrm{Res1} = \frac{QRT_\mathrm{i}^2}{n^2 E} \quad \text{and}$$
$$\mathrm{Res2} = 2 * \left\{1 - \frac{1}{n^2} + n \ln\left[\frac{T_\mathrm{i}^2 RK(T_\mathrm{i})}{\beta E}\right]\right\}\frac{RT_\mathrm{i}}{E}, \tag{8}$$

where

$$Q(T_p) = 2\left|\frac{\frac{dp_1}{dT} - \frac{dp_0}{dT}}{p_1 - p_0}\right| T_i. \quad (9)$$

If both residuals are neglected in Eq. 7 (see appendix), the data points in a plot of the $\ln\beta/T_i^2$ versus $1/T_i$ (Kissiger-like plot) are approximated by a straight line, from the slope of which a value for the effective activation energy, $E$, is obtained [12, 19]. We settle that with the definition of the state variable $\theta$ (c.f. Refs. [6, 13]), the adoption of a specific model of reaction is not a necessary condition to obtain the effective activation energy from the slope of a Kissinger-like plot.

An analytical solution of the KJMA rate equation for the general non-isothermal case at constant heating rate, assuming that the nucleation (N) and growth (G) rates have an Arrhenius dependence of temperature has been published [20]:

$$\xi = 1 - \exp\left\{-\left[K_0 C \frac{E}{\beta R} P\left(\frac{E}{RT}\right)\right]^n\right\}, \quad (10)$$

where it is considered that the transformation rate is negligible at the initial temperature of the experiment.

In this expression, $P(E/RT)$ is the exponential integral, and $C$ a constant that depends on $n$, $E_N$ and $E_G$ (activation energies for nucleation and growth mechanisms, respectively) [20]. The constant $C$ reduces to unity in particular situations when the nucleation is completed prior to crystal growth (site saturation situation) or in the isokinetic situation where $E_N = E_G$ [20].

In order to obtain a suitable Kissinger-like plot ($\ln[\beta/T_p^2]$ versus $1/T_p$), Eq. 2 is substituted into Eq. 1, and taking into account that the peak temperature $T_p$ (usual in calorimetric experiments) is determined by the condition $\left[d^2\xi/dt^2\right]_{T_p} = 0$, the authors [20], without recourse to any kinetic model, obtained the relation:

$$\ln\left[\frac{\beta}{T_p^2}\right] = -\frac{E}{R * T_p} + \ln\left[-\frac{RK_0 C g'(\xi_p)}{E}\right]. \quad (11)$$

As a KJMA kinetic model is assumed, then:

$$g(\xi) = n(1-\xi)[-\ln(1-\xi)]^{\frac{n-1}{n}} \quad \text{and}$$
$$g'(\xi) = \frac{dg}{d\xi} = \frac{g(\xi)}{1-\xi} + \frac{n-1}{[-\ln(1-\xi)]^{\frac{1}{n}}}. \quad (12)$$

It has been demonstrated that in the peak temperature $\xi_P = 0.632$ and, therefore, $g'(\xi_{T_p}) = -1$ [20]. Equation 11 can be now applied to the non-isothermal dilatometry data at temperatures $T_i$, corresponding to the inflection points for different constant heating rates (the temperatures $T_i$ belong with very good approximation to an equivalent stage of the reaction, $\xi_{T_i} = 0.632$). It is well recognized in the literature [6] that the temperature of the maximal transformation rate ($T_p$ in calorimetric experiments) can be replaced by the temperature of the same degree of transformation $T_\xi$, and that in non-isothermal dilatometric curves at different heating rates can be replaced with a very good approximation by $T_i$.

Then, as it can be seen, Eq. 11 coincides with Eq. 7 in the isokinetic case ($E_N = E_G$), or in the site saturation situation ($C = 1$), if both residuals in Eq. 7 are neglected.

In order to calculate the parameters $K_0$ and $C$ a non-linear regression analysis is performed using Eq. 11 where $T_p$ has been changed by $T_i$ and $g'(\xi_{T_p}) = -1$ at the inflection points. Consequently, it is possible to obtain a transcendent equation to find $n$ through the second derivative of Eq. 10:

$$-n(K_0C)^n\left(\frac{E}{\beta R}\right)^{n-1}\left(p\left(\frac{E}{RT_i}\right)\right)^n \exp\left(-\frac{E}{RT_i}\right)$$
$$+(n-1)\frac{\beta R}{E}\exp\left(-\frac{E}{RT_i}\right) + \frac{\beta E p\left(\frac{E}{RT_i}\right)}{RT_i^2} = 0. \quad (13)$$

An alternative method to estimate the effective activation energy and other kinetic parameters directly from the non-isothermal dilatometry curves is presented in [14]. Furthermore, this procedure allows analyzing if the effective activation energy, obtained by the above Kissinger-like plot, is constant during the entire transformation. For this, the fraction untransformed $(1-\xi)$, according to Eq. 4 with $p = \Delta l/l$ (relative change of length), is defined as:

$$(1-\xi) = \left[\left(\frac{\Delta l(T)}{l}\right)_T - \left(\frac{\Delta l(T)}{l}\right)_{end}\right] \Big/ \left[\left(\frac{\Delta l(T)}{l}\right)_0 - \left(\frac{\Delta l(T)}{l}\right)_{end}\right], \quad (14)$$

where $(\Delta l(T)/l)_0$ and $(\Delta l(T)/l)_{end}$ are the relative length increments of the start and end stages, respectively, at temperature $T$. The $(\Delta l(T)/l)_T$ is the relative length increment on dilatometric curve at temperature $T$, as it is depicted in Fig. 1. According to this definition $(1-\xi) = 1$ and $\xi = 0$ at the start temperature of the transformation $T = T_s$.

This procedure was applied to nucleation and growth reactions (tempering reactions in steels) using an expression oversimplified for $g(\xi) = (1-\xi)^{n_0}$ [14]. This way, the analysis is based on the assumption of homogeneous reactions with a reaction rate:

$$-\frac{d(1-\xi)}{dt} = K(1-\xi)^{n_0} \quad (15)$$

where the order of the tempering reaction under consideration is $n_0$.

Differentiation of Eq. 15 (with $\beta$ as a constant and $K = K_0\exp(-E/RT)$), and its evaluation at the inflection point temperature ($T_i$) on the curve $(1-\xi)$ versus

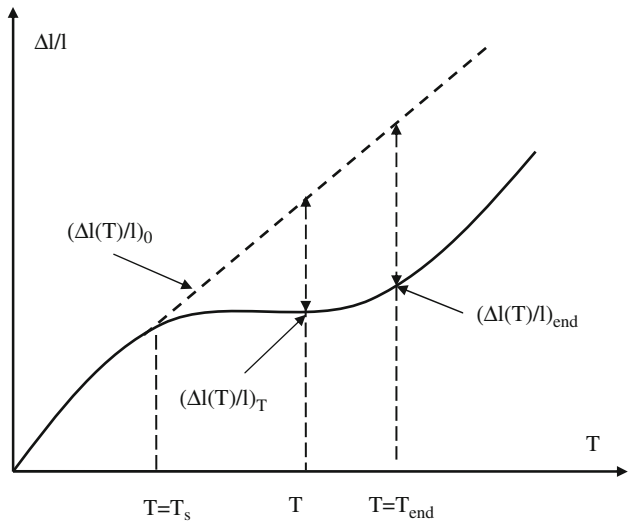


**Fig. 1** Relative length change ($\Delta l(T)/l$) near the inflection point according to [14]

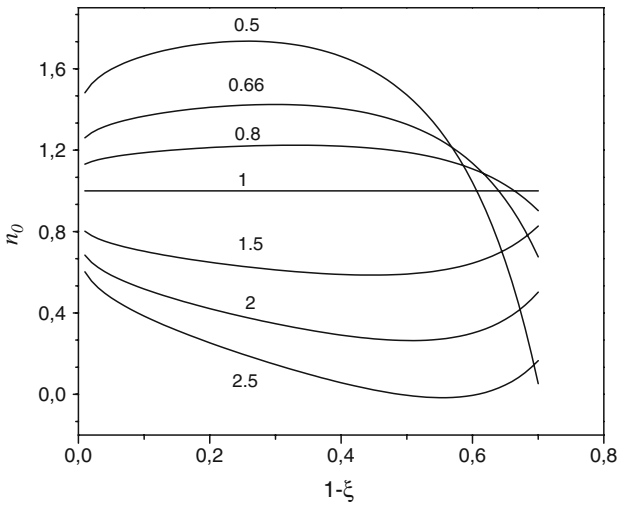


**Fig. 2** Behavior of the $n_0$ parameter versus the fraction untransformed $(1 - \xi)$ for different Avrami exponent values

temperature, the equation for the effective activation energy is obtained:

$$E = -\frac{n_0 R T_i^2 (1-\xi)_{T_i}^{n_0-1} \left.\frac{d(1-\xi)}{dT}\right|_{T_i}}{(1-\xi)_{T_i}^{n_0}}. \quad (16)$$

The other kinetic parameters can be calculated through the equations:

$$K_0 = -\frac{\beta}{(1-\xi)_{T_i}^{n_0}} \left.\frac{d(1-\xi)}{dT}\right|_{T_i} \exp\left(\frac{E}{RT_i}\right), \quad (17)$$

and

$$(1-\xi)_T^{n_0} = -\frac{\beta}{K_0}\left(\frac{d(1-\xi)}{dT}\right)_T \exp\left(\frac{E}{RT}\right). \quad (18)$$

Although the above simplification could be questioned, this approximation may be used to investigate the variation of the effective activation energy under different experimental conditions [21]. In order to solve this difficulty it is assumed that the tempering reactions obey a KJMA kinetic model. Therefore, if the above formalism for homogeneous transformations is settled; then, a relationship between the Avrami exponent $n$ and the kinetic order of the reaction $n_0$ can be obtained as a function of the fraction untransformed $(1 - \xi)$. Thus, the transformation rate for a reaction that obeys a KJMA relation is:

$$-\frac{d}{dt}(1-\xi) = K(1-\xi)\, n\, (-\ln(1-\xi))^{\frac{n-1}{n}}. \quad (19)$$

From the Eqs. 15 and 19, the expression that related $n$, $n_0$ and $(1 - \xi)$ resulted to be:

$$n_0 = 1 + \frac{\ln[n\,(-\ln(1-\xi))^{\frac{n-1}{n}}]}{\ln(1-\xi)}. \quad (20)$$

As it is shown in Fig. 2, the behavior of the $n_0$ function depends weakly on $(1 - \xi)$ far from the boundary point $(1 - \xi) = 1$. As a consequence, $n_0$ can be considered as a constant during the development of the reaction for stages where the fraction transformed is greater than 0.4. Also, the $n_0$ values are lower the greater the Avrami exponent, and when the Avrami exponent takes the value $n = 1$, the reaction is the first order ($n_0 = 1$). Evaluation of $n_0$ from the different nucleation and growth protocols, given by the $n$ values, makes possible to use the procedure established in [14] to nucleation and growth reactions and therefore to determine if $E$ is constant during the entire transformation. For this, the fraction untransformed values calculated from Eq. 18 (where it is used the $E$ value determined by a Kissinger-like plot) for the entire reaction are compared with the experimental fraction untransformed data obtained from the dilatometric curve.

The Friedman-like methods conceived to be used in processing of non-isothermal calorimetric data do not require any mathematical approximation to solve the temperature or exponential integral [1, 10]. This procedure allows obtaining the activation energy of a reaction knowing the reaction rates at a stage with the same degree of transformation for various heating rates. According to the knowledge of the present authors, the Friedman-like methods have not been very much used with non-isothermal dilatometry data.

In fact, if $d\xi/dt$ at temperatures corresponding to the inflection points ($T_i$) is known then, substituting Eq. 2 into 1 ($\beta = dT/dt$), the following equation results after applying logarithms to both terms:

$$\ln\left(\frac{d\xi}{dt}\right)\Big|_{T_i} = \ln\left(\beta\frac{d\xi}{dT}\right)\Big|_{T_i} = -\frac{E}{RT_i} + \ln(K_0 g(\xi_i)). \quad (21)$$

As in the dilatometry record one has that $\left(\frac{\delta l}{l}\right)_t = \frac{l_t - l}{l}$, where $l$ is the initial length of the sample and $l_t$ is the length at any instant, then:

$$\frac{dl_t}{dT} = l\left(\frac{d}{dT}\left(\frac{\delta l}{l}\right)_t\right). \quad (22)$$

Differentiating Eq. 4 with respect to time (with $p = \frac{\delta l}{l}$), it is obtained that:

$$\frac{d\xi}{dt} = \frac{d}{dt}\left(\frac{l_t - l_0}{l_1 - l_0}\right) = \frac{1}{l_1 - l_0}\frac{dl_t}{dt} = h_l\frac{dl_t}{dt} = h_l\beta\frac{dl_t}{dT} = \beta\frac{d\xi}{dT}, \quad (23)$$

where $h_l = \frac{1}{l_1 - l_0}$.

If Eq. 22 is substituted into Eq. 23 and logarithm is applied to both the terms then, at temperatures corresponding to the inflection points, the following relation (after using Eq. 21) can be sustained:

$$\ln\left(\beta\frac{d\xi}{dT}\right)\Big|_{T_i} = \ln(h_l l) + \ln\left(\beta\frac{d}{dT}\left(\frac{\delta l}{l}\right)\Big|_{T_i}\right) = -\frac{E}{RT_i} - \ln(K_0 g(\xi_i)). \quad (24)$$

This equation can also be written as:

$$\ln\left[\beta\frac{d}{dT}\left(\frac{\delta l}{l}\right)\Big|_{T_i}\right] = -\frac{E}{RT_i} + \text{Const.} \quad (25)$$

According to Eq. 25 it is possible to calculate the effective activation energy $E$ (but not the frequency factor, $K_0$).

## Experimental procedure

Commercial plain carbon steel having a carbon content of approximately 0.5 wt% was used for the tempering analysis. The chemical composition of the (AISI 1050) steel is given in Table 1. The test specimens were in the form of rod 2 mm in diameter and 12 mm in length. The specimens were austenitized (900 °C) in a vacuum tube furnace. Austenitising conditions were selected to give complete carbide solution. The quenched treatment was carried out in water at ambient temperature. To obtain the non-isothermal dilatometry records at constant heating rates on the tempering treatment (from ambient temperature up to 600 °C), a dilatometer (Adamel-Lhomargy, model DT 1000, NY, USA) belonging to the Engineering School of the São Paulo University in São Carlos, Brazil, was used.

**Table 1** Chemical composition of the AISI 1050 steel

| C (wt%) | Mn (wt%) | P (wt%) | S (wt%) |
|---|---|---|---|
| 0.48–0.55 | 0.6–0.9 | 0.04 | 0.05 |

The dilatometer was calibrated by means of periodic measurements of the thermal-expansion coefficients of well-known samples, with standard $\Delta l(T)/l$ curves. The relative length changes in the specimen (with an accuracy of $10^{-4}$) against temperature were obtained, while the specimen is heated at a constant rate. The constant heating rates were 5, 10, 15, 20, and 30 K/min.

## Results

Figure 3 shows a non-isothermal dilatometry record at 5°/min as heating rate, where the transformation temperatures for both processes are indicated. Table 2 and Fig. 4 show the temperatures corresponding to the inflection points from the dilatometric curves with different heating rates for both processes. By lineal (see Table 3; Fig. 5) and non-lineal regression analyses using Eq. 7 (neglecting the residues as it is outlined in the appendix), the best $E$ and $K_0$ parameters were calculated for the two identified processes on tempering in the non-isothermal dilatometry records.

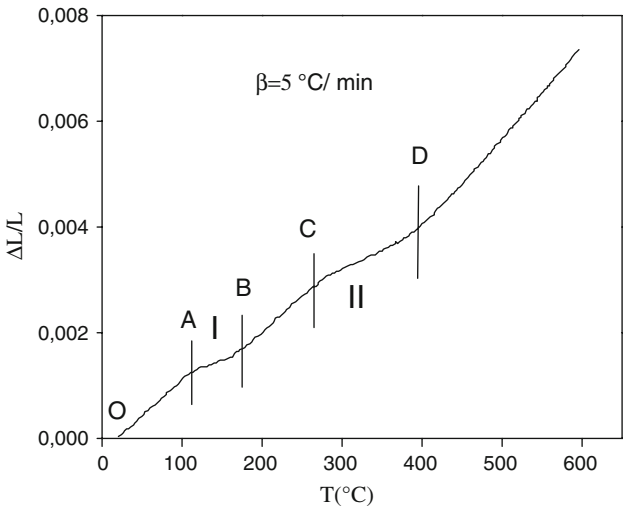


**Fig. 3** Non-isothermal dilatometry record ($\beta = 5$ °C/min) showing the temperature intervals corresponding to both the processes on tempering

**Table 2** Temperatures corresponding to the inflection points ($T_i$) at different heating rates ($\beta$) for processes I and II on tempering in the dilatometry records

| $\beta$ (K/min) | $T_i$ (K) process I | $T_i$ (K) process II |
|---|---|---|
| 5 | 411.6 | 584.3 |
| 10 | 418.9 | 593.5 |
| 15 | 424.3 | 599.1 |
| 20 | 428.5 | 603.1 |
| 30 | 432.4 | 608.8 |

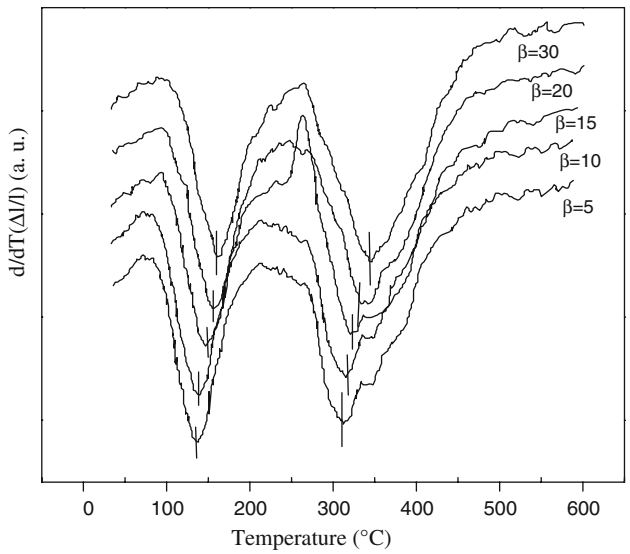


**Fig. 4** The $d(\Delta l(T)/l)/dT$ versus temperature at different heating rates

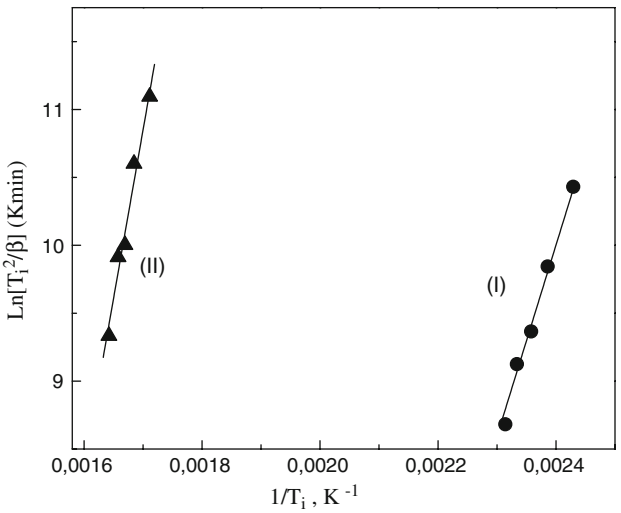


**Fig. 5** Plot of $\ln(T_i^2/\beta)$ versus $(1/T_i)$, where $T_i$ and $\beta$ denote the inflection point temperature and the heating rate, respectively, for the first (I) and second (II) processes on tempering of the AISI 1050 steel

Although one has the possibility, with this procedure (Eqs. 7–9), to obtain a relationship for calculating the Avrami exponent ($n$) of the reaction, we think that the $n$ values are not very reliable due to the many approximations used to obtain the residues. For this reason, the use of the transcendent equation, Eq. 13, is very much reliable to calculate $n$, given by much less approximations in their determination. In this sense, as a first step, the $K_0$ and C parameters are calculated using Eq. 11 by a non-lineal regression analysis where the $E$ value (obtained by a Kissinger-like plot, Eq. 7) is considered as a fixed parameter. The best fitting values for $K_0$ and $C$ parameters, for both processes on tempering, are listed in Table 4, where the statistical parameter $P$ for calculating $C$ is shown. We pointed out that the $P$ values represent the probability that a better fit to the same data can be carried out by another model. Table 5 shows the Avrami exponent for each considered process on tempering at different heating rates solving the transcendent equation, Eq. 13.

The uncertainty showed in each Avrami exponent value ($\delta n$) (Table 5) was calculated by the propagation of the uncertainty [22] in temperature ($\delta T = 0.1$ °C) and in the activation energy ($\delta E = 0.5$ kJ/mol calculated by non-linear regression analysis of Eq. 7) from the transcendent equation $F(n, T, E) = 0$. Thus, as the variables of the function $F$ are provided of an uncertainty, the corresponding uncertainty of the own function is:

$$\Delta F = \frac{\partial F}{\partial n}\delta n + \frac{\partial F}{\partial E}\delta E + \frac{\partial F}{\partial T}\delta T. \tag{26}$$

By applying this result to Eq. 13, considering only the uncertainties $\delta n$, $\delta T$, $\delta E$ and carrying out some algebraic manipulations, the following expression for the uncertainty in the $n$ value is obtained:

$$\delta n = q(E, n, K_0)\delta T + w(E, n, K_0)\delta E, \tag{27}$$

where the explicit forms of these terms are omitted because they are too large. After this, it is concluded that the first

**Table 3** Best parameters $E$ and $K_0$ calculated by linear and non-lineal regression analyses, respectively, for the two processes on tempering using Eq. 7 where both residuals have been ignored

| Process | Activation energy, $E$ (kJ/mol) | Frequency factor, $K_0$ ($min^{-1}$) | Confidence interval for $E$ | Regression coefficient $R$ | P value for $E$ |
|---|---|---|---|---|---|
| I | 117 | $2.99 \times 10^{14}$ | $104 < E < 130$[a]<br>$116.5 < E < 117.4$[b] | 0.998[b] | $4.8 \times 10^{-10}$[b] |
| II | 206 | $9.53 \times 10^{17}$ | $196 < E < 216$[a]<br>$205.6 < E < 206.4$[b] | 0.999[b] | $9.0 \times 10^{-14}$[b] |

$P$ = Distr. T(T, FD, 2): It represents the probability that a better fit to the same data can be carried out by another model. As the $P$ values are very low, it is not very probable that another model fits the data better than the model here shown

[a] Lineal regression analysis

[b] Non-lineal regression analysis ($E$ and $K_0$ are the fitting parameters)

**Table 4** Best parameters, $K_0$ and $C$, determined by non-linear regression analysis using Eq. 11

| | $E$ (kJ/mol) (fixe) | $K_0$ ($min^{-1}$) (fp) | $C$ (fp) | Regression coefficient $R$ | $P$ (only for $C$) |
|---|---|---|---|---|---|
| Process I | 117 | $2.99 \times 10^{14}$ | 1 | 0.997 | 0.00002 |
| Process II | 206 | $9.53 \times 10^{17}$ | 1 | 0.999 | $4 \times 10^{-8}$ |

*fixe* fixed parameter, *fp* fitting parameter

**Table 5** The Avrami exponent for the two processes on tempering

| $\beta$ (K/min) | $T_i$ (K) | $n$ | $\delta n$ |
|---|---|---|---|
| First process on tempering | | | |
| 5 | 411.6 | 1.2 | 0.2 |
| 10 | 418.9 | 1.1 | 0.2 |
| 15 | 424.3 | 1.0 | 0.2 |
| 20 | 428.5 | 1.1 | 0.2 |
| 30 | 432.4 | 1.0 | 0.2 |
| Second process on tempering | | | |
| 5 | 584.3 | 0.7 | 0.1 |
| 10 | 593.5 | 0.7 | 0.1 |
| 15 | 599.1 | 0.7 | 0.1 |
| 20 | 603.1 | 0.7 | 0.1 |
| 30 | 608.8 | 0.7 | 0.1 |

**Table 6** Activation energies ($E$) and the frequency factors ($K_0$) for the first process on tempering using Eqs. 16 and 17

| $\beta$ | $T_i$ (K) | $n_0$ | $K_0$ ($min^{-1}$) | $E$ (kJ/mol) | $\delta E$ (kJ/mol) |
|---|---|---|---|---|---|
| 5 | 411.6 | 1.0 | $5.4 \times 10^{14}$ | 119 | 6 |
| 10 | 418.9 | 1.0 | $6.87 \times 10^{13}$ | 112 | 6 |
| 15 | 424.3 | 1.0 | $3.3 \times 10^{14}$ | 117 | 6 |
| 20 | 428.5 | 1.0 | $2.0 \times 10^{15}$ | 124 | 7 |
| 30 | 432.4 | 1.0 | $1.1 \times 10^{14}$ | 113 | 6 |

**Table 7** Activation energies ($E$) and the frequency factors ($K_0$) for the second process on tempering using Eqs. 16 and 17

| $\beta$ | $T_i$ (K) | $n_0$ | $K_0 \times 10^{17}$ ($min^{-1}$) | $E$ (kJ/mol) | $\delta E$ (kJ/mol) |
|---|---|---|---|---|---|
| 5 | 584.3 | 1.4 | 1.3 | 196 | 11 |
| 10 | 593.5 | 1.4 | 1.2 | 196 | 10 |
| 15 | 599.1 | 1.4 | 1.3 | 196 | 10 |
| 20 | 603.1 | 1.4 | 1.6 | 197 | 10 |
| 30 | 608.8 | 1.4 | 1.3 | 196 | 10 |

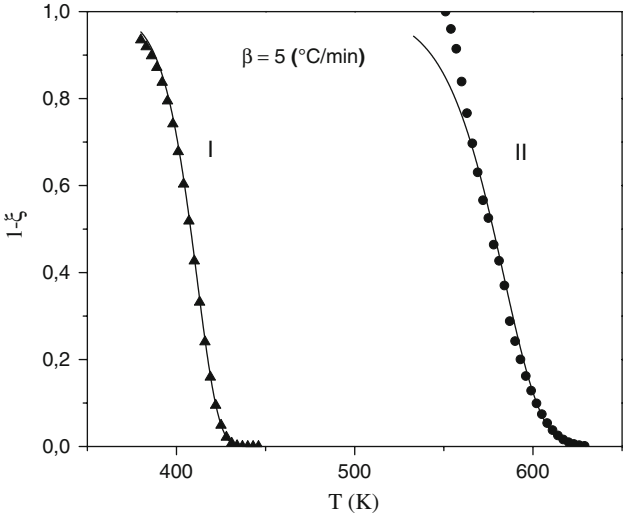


**Fig. 6** Fraction untransformed versus temperature according to Eq. 18: Experimental curves for the first (I) and second (II) processes with a heating rate: $\beta = 5$ °C/min. The symbols: *filled triangle* and *filled circle* are the fraction untransformed values calculated by Eq. 18 for different temperatures. Process (I): $K_0 = 5.4 \times 10^{14}$ $min^{-1}$, $E = 119$ kJ/mol, $n_0 = 1$, $d(1-\xi)/dT|_{T_i} = 0.032275$. Process (II): $K_0 = 1.3 \times 10^{17}$ $min^{-1}$, $E = 196$ kJ/mol, $n_0 = 1.4$, $d(1-\xi)/dT|_{T_i} = 0.0184273$

process on tempering considered by us corresponds to a reaction with $n_0 = 1$ according to the formalism showed in [14]. On the contrary, the second process (third stage of tempering) that in the literature is identified as the cementite precipitation, the $n_0$ parameter has a value close to 1.4 ($n = 0.66$) according to Eq. 20.

Taking the above $n_0$ values for the first and second processes, the new $E$ values at temperatures of the inflection points can be determined by Eq. 16. As can be seen in Tables 6 and 7, these values are the same, within the error boundary, as those obtained by a Kissinger-like plot. The frequency factors for each heating rate are calculated using Eq. 17. In Tables 6 and 7, the parameters obtained by the expressions (16) and (17) are shown.

According to Eq. 18, the fraction untransformed values are calculated for the entire range of temperatures using the determined $E$, $K_0$, and $n_0$ values. Only for the above $n_0$ values, the calculated effective activation energy is constant for the entire reaction, Fig. 6. Other nucleation and growth protocols that generate another $n_0$ values (see Fig. 2) cause appreciable deviations among the experimental and calculated fraction untransformed values for the range of temperatures where the reactions are developed.

Tables 8 and 9 show the $d/dT(\delta l/l)$ data at temperatures corresponding to the inflection points, for both processes on tempering. These data are used in the determination of the effective activation energy by a Friedman-like procedure. By linear fitting of Eq. 25, the effective activation

**Table 8** $d/dT(\delta l/l)_{T_i}$ at different heating rates for the first process on tempering

| $\beta$ | $T_i$ (K) | $d/dT(\delta l/l)_{T_i} \times 10^{-6}$ |
|---|---|---|
| 5 | 411.6 | 4.43 |
| 10 | 418.9 | 4.95 |
| 15 | 424.3 | 4.46 |
| 20 | 428.5 | 4.49 |
| 30 | 432.4 | 4.95 |

**Tabla 9** $d/dT(\delta l/l)_{T_i}$ at different heating rates for the second process on tempering

| $\beta$ | $T_i$ (K) | $d/dT(\delta l/l)_{T_i} \times 10^{-6}$ |
|---|---|---|
| 5 | 584.3 | 5.08 |
| 10 | 593.5 | 5.6 |
| 15 | 599.1 | 5.35 |
| 20 | 603.1 | 4.8 |
| 30 | 608.8 | 4.74 |

energy was for both processes: $E = 127.5$ kJ/mol, $\delta E = 32.7$ kJ/mol (first process) and $E = 202.9$ kJ/mol, $\delta E = 40$ kJ/mol (second process), very close to those determined by a Kissinger-like method.

## Discussion

Considering the chemical composition of steel and the results obtained by the analysis of the dilatometry records, it is assumed that the new nuclei corresponding to the first stage of tempering could have been formed during the quench. This is because in the studied steel, the $M_s$ temperature (martensite start temperature) is closed to 300 °C according to the $M_s$ relation for 0.5 wt% C and 0.8 wt% Mn [23], and by the greater mobility of the carbon atoms through the dislocations inherited from the martensite structure [24].

The lineal behavior observed in the dilatometric curves from room temperature up to approximately 110 °C is mainly due to the thermal dilation on heating of the steel (see right line of the curve indicated by OA in Fig. 3).

In the temperature range of approximately 100–200 °C (see Figs. 3, 4) for the first processes at the non-isothermal dilatometric registers, the transition carbide (epsilon carbide) nuclei that have been formed on quenching are growing. The growth of the transition carbide produces a lost of tetragonality of the martensite matrix by the exit of the interstitial carbon in solution. This is the cause of the inflection in the dilatometry record (first process (I), AB interval in Fig. 3). The above is in agreement with the situation where existing nuclei in form of needles or plates are developed by controlled diffusion growth corresponding to the Avrami exponent close to one ($n = 1$)[25] as it is shown in Tables 4 and 5 for this first process on tempering. As it can be appreciated in processes (I and II) on tempering, the nucleation and growth mechanisms are quite separated (site saturation situation); since, the coefficient C in Eq. 11 resulted to be $C = 1$ by the non-linear regression analysis above discussed. The growth reaction of the transition carbide is corresponded with a parameter $n_0 = 1$, according to Eq. 20 where the Avrami index resulted to be $n = 1$ (see Table 6).

The effective activation energy found for the first process from the non-isothermal dilatometry records using the most accepted isoconversion methods was among 117–128 kJ/mol. These values are in agreement with the one reported by [19, 26] for diffusion of the iron atoms along dislocations that are generated by the incoherency between the transition carbide and the matrix. Therefore, it will be the diffusion of the iron atoms and not the carbon atoms diffusion that control the reaction during this first process on tempering. In Fig. 6, the curve (I) shows that the fraction untransformed values calculated using Eq. 18 during the ongoing reaction are in agreement with the fraction untransformed values determined from the dilatometric record for the same interval of the transformation temperatures (experimental curve in Fig. 6). Thus, the effective activation energy obtained as the slope of a Kissinger-like plot is not only valid for the temperature corresponding to the inflection point, but also for the whole interval of temperatures where this reaction occur. For this reason, we assume that $E = E_G$ is constant for this first precipitation process on tempering.

For temperatures from 170 to 300 °C, when the transformation (I) concludes, it is well established that the retained austenite ($\gamma_r$), with approximately 4% in volume, transforms into cementite ($\theta$) and bainitic ferrite ($\alpha$) [27]. This process should increase the volume of the sample; however, as the amount of the retained austenite is small, the respective change in the volume of the sample is difficult to appreciate in the dilatometry curves (BC in Fig. 3) and it is not considered by us.

In the temperature range ($\sim$300–350 °C), process (II), the transition carbide is dissolved to form cementite. This process should originate a contraction of volume that it is appreciated in the dilatometric curve (CD in Fig. 3). While the cementite particle grows, the transition carbide particles should disappear gradually, due to the iron atoms diffusion along dislocations to form the cementite. The decomposition processes of retained austenite and the transition carbide are generally overlapped, but as the amount of retained austenite is very small, it is assumed that the reduction of volume during the second process is due, practically, to the nucleation and growth of the

cementite on dislocations near of the transition carbide. The above is supported by the fact that the Avrami exponent is close to 0.66 for this second process (third stage of tempering) (see Table 5). This value is in correspondence with the protocol where the nuclei (cementite) are formed at dislocations and the growth is controlled by diffusion of the iron atoms [25]. This last statement is argued by the value of the effective activation energy calculated for this second process, which resulted to be close to 200 kJ/mol. This intermediate value of the activation energy between 134 and 251 is in correspondence with the combination of the pipe diffusion of the iron atoms [19, 26], and of the volume diffusion of the iron atoms in ferrite [19, 28]. This could suggest a new distribution of the iron atoms to form the cementite by dissolution of the transition carbide.

As it can be seen in Table 7, this second process is a tempering reaction with the $n_0$ parameter close to 1.4. This values is different to the one reported by [29] for the third stage of tempering. Also for this second process, according to the calculated kinetic parameters ($n_0$ and $K_0$), the effective activation energy is constant during the entire transformation as it is shown in Fig. 6, curve (II).

## Conclusions

The kinetics of the precipitation reactions that takes place during the first and third stages on tempering were characterized by non-isothermal dilatometry experiments. In this sense, the kinetic parameters as effective activation energy, the frequency factor and the Avrami exponent were calculated by some procedures adapted to non-isothermal dilatometry experiments. The main features of these reactions on tempering in the AISI 1050 steel were:

- The first stage was predominantly a growth reaction of the transition carbide formed during quenching. This growth reaction is controlled by the diffusion of the iron atoms through the dislocations of the martensitic structure.
- The third stage on tempering takes place by progressive nucleation of cementite on dislocations of the structure as consequence of the dissolution of the transition carbide. This reaction is also controlled by the diffusion of the iron atoms through the defects (high density of dislocations) and in the volume of the ferrite matrix.

It is pointed out that through the above recipes it can be determined if the effective activation energy is constant during the ongoing tempering transformation.

**Acknowledgements** The authors wish to thank Dr. M. LLanes for reading through the manuscript. They also wish to thank Engineering School of the University of São Paulo in São Carlos, Brazil by the dilatometry experiments and Coordenação de Aperfeiçoamento de Pessoal de Nivel Superior (CAPES) in Brazil for the financial support offered by the project CAPES-MES/Cuba No. 046/08.

## Appendix

To calculate the value of the residuals, Res1 and Res2 in Eq. 7, it is necessary to calculate the value of the parameter $Q(T_i)$. In this case, the parameter $p$ is the length of the sample l:

$$Q(T_i) = 2\,\frac{\frac{dp_1}{dT} - \frac{dp_0}{dT}}{p_1 - p_0} = 2\frac{(\alpha_1 l_1 - \alpha_0 l_0)}{l_1 - l_0} \cong \frac{\Delta\alpha}{\frac{\Delta l}{l_0}} \tag{28}$$

where $\alpha_0$ and $\alpha_1$ are the coefficients of lineal expansion of the sample before and after the transformation, respectively. For structures containing more than one phase, the next relationship is verified [30]:

$$\alpha = \alpha_1 V_1 + \alpha_2 V_2 + \alpha_3 V_3 + \cdots, \tag{29}$$

where $\alpha_i$ and $V_i$ are, respectively, the coefficient of lineal expansion and the volumetric fraction of the phase $i$. Before starting the transformation, see segment OA in Fig. 3, Eq. 29 can be written as:

$$\alpha_0 = \alpha_m V_m + \alpha_{ar} V_{ar}, \tag{30}$$

and after the transformation corresponding to the process (I):

$$\alpha_1 = \alpha_c V_c + \alpha_{fe} V_{fe} + \alpha_{ar} V_{ar} \tag{31}$$

where the subindexes (m, ar, c, fe) refer to the martensite (m), retained austenite (ar), transition carbide (c), and ferrite (fe). It should also be certain that:

$$V_m + V_{ar} = 1, \quad V_c + V_{fe} + V_{ar} = 1. \tag{32}$$

The transformation that causes a volume change during the first process is:

$$(\ \alpha' + \gamma_r \rightarrow \alpha + \varepsilon\ + \gamma_r\ )$$

where we have considered to the transition carbide-like epsilon carbide $\varepsilon$. The $\alpha'$ and $\gamma_r$ are the martensite and retained austenite phases, respectively.

According to this reaction, it is possible to calculate the volumetric fraction of the transition (epsilon) carbide, $V_c$, following the next considerations: If we call to $N^c$, $N^{fe}$, and $N^m$ the number of the iron atoms in the epsilon carbide, ferrite, and martensite phases, respectively, and $v^c$, $v^{fe}$, and $v^m$ the volumes of an iron atom in these phases, then by substance conservation the following relationship is sustained:

$$\frac{\Delta V}{V} = 3\frac{\Delta l}{l_0} = \frac{N^c v^c + N^{fe} v^{fe} + N^{ar} v^{ar} - (N^c v^m + N^{fe} v^m + N^{ar} v^{ar})}{N^m v^m}. \tag{33}$$

If $y = \frac{N^c}{N^m}$ is the fraction of iron atoms that have been transformed in epsilon carbide, the relationship (33) can be written as:

$$\frac{\Delta V}{V} = 3\frac{\Delta l}{l_o} = \frac{y(v^c - v^m) + (1-y)(v^{fe} - v^m)}{v^m} \quad (34)$$

But, the volumetric fraction of epsilon carbide that has been formed is:

$$V_c = \frac{N^c v^c}{N^m v^m} = y\frac{v^c}{v^m}. \quad (35)$$

According to definition $y$ and Eq. 34 it is obtained:

$$V_c = \frac{N^c v^c}{N^m v^m} = y\frac{v^c}{v^m} = \left\{\frac{\left(3\frac{\Delta l}{l_0} + 1\right)v^m - v^{fe}}{v^c - v^{fe}}\right\}\frac{v^c}{v^m}. \quad (36)$$

In this relation $\Delta l/l_0$ is calculated from the dilatometry record by extrapolation up to the inflection point. The $v^c$, $v^{fe}$, and $v^m$ values and those of $\alpha_i$ are obtained from the literature [19]:

$$v^m = 11.9593\,A^3/Fe(0.5\%\,C) \quad \alpha_m = 11.5 * 10^{-6}\,^\circ C^{-1}$$
$$v^{fe} = 11.77\,A^3/Fe \quad \alpha_{fe} = 14.5 * 10^{-6}\,^\circ C^{-1};$$
$$\alpha_{ar} = 23 * 10^{-6}\,^\circ C^{-1}$$
$$v^c = 13.827\,A^3/Fe \quad \alpha_c = \alpha_\theta = 12.5 * 10^{-6}\,^\circ C^{-1}$$

In Table 10, the values of the $Q$ parameter, calculated for each dilatometry curve corresponding to the first process, are shown. The volumetric fraction of the epsilon carbide, $V_c$, is calculated using the Eq. 36 and the volumetric fraction of ferrite, $V_{fe}$, is calculated using Eq. 32. The volumetric fractions of martensite and the retained austenite are in all cases: $V_m = 0.96$, $V_{ar} = 0.04$, respectively.

It is appreciated that the $Q$ parameter is approximately $-0.01$ for the first process on tempering.

For the second process II (third stage of tempering), the parameter is $Q = 0$. In this sense, the following reaction, during this second process, is manifested:

$$(\varepsilon \rightarrow \theta', \alpha + \varepsilon + \theta \rightarrow \alpha + \theta + \theta'),$$

where $\theta$ and $\alpha$ are the cementite and ferrite phases, respectively. The cementite from the transition carbide (epsilon carbide) is $\theta'$. Thus,

**Table 10** $Q$ values for the first process

| $\beta$ | $\Delta l/l_0 \times 10^{-4}$ | $V_c$ (%) | $V_{fe}$ (%) | $\alpha_1 \times 10^{-6}$ | $\alpha_0 \times 10^{-6}$ | $Q \times 10^{-2}$ |
|---|---|---|---|---|---|---|
| 5 | −4.2 | 9.8 | 86.2 | 14.5 | 11.8 | −1.3 |
| 10 | −3.86 | 9.9 | 86.1 | 14.5 | 11.8 | −1.6 |
| 15 | −4.52 | 9.7 | 86.3 | 14.5 | 11.8 | −1.3 |
| 20 | −4.4 | 9.8 | 86.2 | 14.5 | 11.8 | −1.1 |
| 30 | −4.5 | 9.7 | 86.3 | 14.5 | 11.8 | −1.1 |

**Table 11** Process (I): $E = 117$ kJ/mol, $n = 1$, $K_0 = 2.99 \times 10^{14}$ min$^{-1}$, $Q = -0.01$, ln $K_0R/E = 23.7$ (min K)$^{-1}$; process (II): $E = 206$ kJ/mol, $K_0 = 9.5 \times 10^{17}$, $n = 0.66$, $Q = 0.0$, Res1 = 0.0, ln $K_0R/E = 31$ (min K)$^{-1}$

| $\beta$ | Process (I) | | | | Process (II) | | |
|---|---|---|---|---|---|---|---|
| | $T_i$ (K) | Res1 | Res2 | $RT_i/E$ | $T_i$ (K) | Res2 | $RT_i/E$ |
| 5 | 411.6 | 0.12 | 0.00018 | 0.029 | 584.3 | −0.061 | 0.023 |
| 10 | 418.9 | 0.124 | −0.0035 | 0.029 | 593.5 | −0.0627 | 0.023 |
| 15 | 424.3 | 0.128 | −0.00067 | 0.03 | 599.1 | −0.063 | 0.024 |
| 20 | 428.5 | 0.13 | 0.0028 | 0.03 | 603.1 | −0.064 | 0.024 |
| 30 | 432.4 | 0.13 | −0.0027 | 0.03 | 608.8 | −0.064 | 0.024 |

$$\alpha_0 = V_{fe}\alpha_{fe} + \alpha_c V_c + \alpha_\theta V_\theta \quad \text{and}$$
$$\alpha_1 = V_{fe}\alpha_{fe} + V_\theta\alpha_\theta + \alpha_{\theta'}V_{\theta'}.$$

In this way $\Delta\alpha = \alpha_1 - \alpha_0 = \alpha_{\theta'}V_{\theta'} - V_c\alpha_c = 0$ because $V_c = V_{\theta'}$ and $\alpha_{\theta'} = \alpha_c$, then $Q = 0$.

Finally the residual Res1 and Res2 values for both processes are shown in Table 11.

## References


1. Starink MJ (2003) Thermochim Acta 404:163
2. Koga N, Sestak J, Malek J (1991) Thermochim Acta 188:333
3. Malek J, Criado JM (1990) Thermochim Acta 164:199
4. Flynn JH (1992) Thermochim Acta 203:519
5. Vyazovkin S (2000) Thermochim Acta 355:155
6. Mittemeijer EJ (1992) J Mater Sci 27:3977. doi:10.1007/BF01105093
7. Kissinger HE (1956) J Res Natl Bur Stand 57:217
8. Kissinger HE (1957) Anal Chem 29:1702
9. Órfáo JJM (2007) AIChE J 53:2905
10. Friedman HL (1964) J Polym Sci C6:183
11. Sewry JD, Brown ME (2002) Thermochim Acta 390:217
12. Mittemeijer EJ, Van Gent A, Van der Schaaf PJ (1986) Metall Trans A 17A:1441
13. Liu F, Sommer F, Bos C, Mittemeijer EJ (2007) Int Mater Rev 52:193
14. Tomita Y (1989) J Mater Sci 24:731. doi:10.1007/BF01107467
15. Robson JD (1996) Modelling of carbide and laves phase precipitation in 9–12 wt% chromium steels. Ph.D. Thesis, University of Cambridge, p 31
16. Kolmogorov AN (1937) Izv Akad Nauk USSR Ser Matemat 1:355
17. Johnson WA, Mehl RF (1939) Trans AIME 135:416
18. Avrami M (1939) J Chem Phys 7:1103
19. Cheng L, Brakman CM, Korevaar BM, Mittemeijer EJ (1988) Metall Trans A 19A:2415
20. Farjas J, Roura P (2006) Acta Mater 54:5573
21. Sestak J, Brown A, Rihak V, Berggren G (1969) Thermal analysis. Academic Press, New York, p 1035
22. Morales EV, Vega LJ, Villar CE, Antiquera MJ, Fadragas RC (2005) Scripta Mater 52:217
23. Stevens W, Haynes AG (1956) J Iron Steel Inst 183:349
24. Hirotsu Y, Nagakura S (1972) Acta Metall 20:645
25. Christian JW (1975) The theory of transformations in metals and alloys. Pergamon Press, Oxford, p 542 (Part 1, Chapter 12)
26. Cohen M (1970) Trans JIM II:145

27. Honeycombe RWK (1981) Steels microstructure and properties. Edward Arnold Editions, London, p 142 (Chapter 8)
28. Buffington FS, Hirano K, Cohen M (1961) Acta Metall 9:533
29. Tomita Y (1988) Mater Sci Technol 4:977
30. Livshits BG, Kraposhin VS, Linetski YaL (1982) Physical properties of metals and alloys. Mir Ed, Moscow, p 381 (Chapter 6)